King Saud University

Journal of Saudi Chemical Society

www.ksu.edu.sa
www.sciencedirect.com

ORIGINAL ARTICLE

Investigation of coupling dehydrogenation and hydrogenation reactions in a fixed bed catalytic reactor with well-mixed catalyst pattern

M.E.E. Abashar *

Chemical Engineering Department, College of Engineering, King Saud University, P.O. Box 800, Riyadh 11421, Saudi Arabia

Abstract   The enhancement of ethylbenzene conversion by further displacement of the thermodynamic equilibrium via the influence of the dual-functionality of a well-mixed catalyst pattern has been investigated. A rigorous steady state mathematical model based on the dusty gas model is implemented for the simulation. The simulation results reveal that the introduction of the concept of the reaction coupling has significant effect on the displacement of the thermodynamic equilibrium and considerable enhancement of simultaneous production of styrene and cyclohexane. Almost 100% conversion of the ethylbenzene and benzene is achieved through the application of this approach. It is also found that considerable decrease in the reactor length is achieved by employing a reactor catalyst bed with different bed compositions. Effective operating regions with optimal conditions are observed. An effective reactor length criterion is used to evaluate the performance of the reactor under these optimal conditions. The effective reactor length is found to be sensitive and favored by high feed temperature and pressure. The sensitivity analysis shows that the key parameters of feed temperature, pressure, and the bed composition play an important role on the reactor performance. The results also show that almost 100% conversion of ethylbenzene and benzene at low temperature and shorter reactor length can be achieved by maintaining the reactor beds

Production and hosting by Elsevier

ELSEVIER

Nomenclature

A	catalyst bed cross-sectional area, m^2
C_i	concentration of component i, kmol/m^3
d_p	catalyst particle diameter, m
$D^e_{k_i}$	Knudsen diffusivity of component i, m^2/s
D^e_{ij}	effective molecular diffusivity of component i, m^2/s
D^e_i	effective diffusivity of component i, m^2/s
G^o	mass velocity of the gas mixture, kg/m^2 s
g_c	gravitational acceleration, m^2/s
F_i	molar flow rate of component i, kmol/s
k_1	reaction 1 rate constant, kmol/kg s kPa
k_2	reaction 2 rate constant, kmol/kg s
K_1	equilibrium constant of reaction 1, kPa
K_B	chemisorption equilibrium constant of benzene, kPa^{-1}
l	catalyst pellet coordinate, m
L_c	characteristic length of the catalyst pellet, m
N_i	molar flux of component i, kmol/m^2 s

P_i	partial pressure of component i, kPa
r_j	rate of reaction j, kmol/kg s
S_x	external surface area of catalyst pellet, m^2
T	temperature, K
V_P	volume of catalyst pellet, m^3
X	conversion of component of component i
y	mole fraction
z	reactor length, m
Z	dimensionless reactor length

Greek letters

γ_{ji}	stoichiometric coefficient for species i in reaction j
ε_k	volume fraction of catalyst k
η_j	effectiveness factor of reaction j
μ_G	viscosity of the gas mixture, kg/m s
ρ_i	density of the catalyst i, kg/m^3
ϕ	bed voidage fraction

at different temperatures. This temperature switching policy may result in appreciable energy saving. Moreover, operating the reactor at low temperature protect the catalyst from the excessive temperatures which have destructive effects on the catalysts and the mechanical stability of the reactors. Also, the low temperature operation has significant contribution to the reduction of the operating cost.

1. Introduction

Styrene is one of the most important intermediate products used in many industries such as: polystyrene, unsaturated polyesters, styrene acrylonitrile resin (SAN), styrene-divinylbenzene (S-DVB), styrene-acrylonitrile resin (SAN), styrene butadiene rubber (SBR), styrene-budadiene latex (SBL) and styrene-iso-prene-styrene (SIS) (http://www.en.wikipedia.org/wiki/Styrene). Cyclohexane, on the other hand, is used in industry to manufacture: nylon fibre, nylon molding resin, solvents for paint, resins, varnish and oils (http://www.en.wikipedia.org/wiki/Cyclohexane).

Styrene is produced commercially from the catalytic dehydrogenation of ethylbenzene (Sheel and Crowe, 1969). The reaction is endothermic and reversible with increasing number of moles. The reaction is severely limited by the thermodynamic equilibrium with a maximum ethylbenzene conversion less than 50% (Dittmeyer et al., 1999). In this case, the styrene production can be favored by low pressure, high temperature and the dilution of the products. There are several ways in which cyclohexane can be produced. The two most common ways are the catalytic hydrogenation of benzene and fractional distillation of petroleum.

In recent years, the subject of multifunctional reactors has received much attention. Examples of multifunctional reactor are spatially or well-mixed catalyst patterns in fixed bed catalytic reactors (Cote et al., 1999) and membrane reactors (Abdalla and Elnashaie, 1993; Becker et al., 1993; Gobina et al., 1995; Moustafa and Elnashaie, 2000; Abashar, 2002a,b; Abashar et al., 2002). The purpose of these patterns (either physically mixed or layered) is to introduce dual-functionality, i.e., to introduce auxiliary reactions for the displacement of the thermodynamic equilibrium, heat integration between exothermic and endothermic and production of more than one product. Despite the evidence of the catalyst patterns benefits, still these configurations are not fully understood and the technology is not commercially utilized.

The aim of this study is to explore the displacement of the thermodynamic equilibrium and the enhancement of the ethylbenzene and benzene conversions gained by application of dual-functionality of well-mixed catalyst patterns in a fixed bed catalytic reactor. To achieve this goal a rigorous heterogeneous model based on the dusty gas model is implemented to study the influence of various key parameters that are likely to affect the performance of the reactor.

2. Reaction kinetics

2.1. Primary reaction

The rate expression for dehydrogenation of ethylbenzene:

$$C_8H_{10} \rightleftharpoons C_8H_8 + H_2 \tag{1}$$

is given by (Becker et al., 1993; Gobina et al., 1995; Elnashaie et al., 2001):

$$r_1 = k_1(P_1 - P_2P_3/K_1), \quad \text{kmol/kg s} \tag{2}$$

2.2. Auxiliary reaction

The rate expression for hydrogenation of benzene:
$$C_6H_6 + 3H_2 \rightarrow C_6H_{12} \tag{3}$$

is given by (Marangozis et al., 1979):

$$r_2 = k_2 K_B \frac{P_3 P_4}{(1 + K_B P_4)(P_3 + P_4)}, \quad \text{kmol/kg s} \tag{4}$$

where P_1, P_2, P_3 and P_4 are partial pressures (kPa) of ethylbenzene, styrene, hydrogen and benzene, respectively.

The rate and equilibrium constants are given by:

$$k_1 = 0.01 \times \exp\left(0.851 - \frac{10931.76}{T}\right), \text{kmol/kg s kPa} \tag{5}$$

$$k_2 = 121.11 \times \exp\left(-\frac{6038.65}{T}\right), \quad \text{kmol/kg s} \tag{6}$$

$$K_1 = 100.0$$
$$\times \exp\left(-\frac{122725.157 - 126.27T - 2.194 \times 10^{-3} T^2}{RT}\right), \quad \text{kPa} \tag{7}$$

$$K_B = 788.0 \times \exp\left(-\frac{3019.32}{T}\right), \quad \text{kPa}^{-1} \tag{8}$$

where T is the absolute temperature (K).

3. Model development

3.1. Bulk gas phase

A rigorous one-dimensional heterogeneous model based on the dusty gas model is developed. This model simulates the operation under steady state and isothermal conditions. Axial diffusion is neglected and the ideal gas behavior is assumed. A schematic diagram of the fixed bed reactor that contains a well-mixed catalyst pattern is shown in Fig. 1.

A differential molar balance on the components gives:

$$\frac{dF_{C_8H_{10}}}{dZ} = -\eta_1 \varepsilon_1 \rho_1 A(1-\phi)zr_1 \tag{9}$$

$$\frac{dF_{C_8H_8}}{dZ} = \eta_1 \varepsilon_1 \rho_1 A(1-\phi)zr_1 \tag{10}$$

$$\frac{dF_{H_2}}{dZ} = \eta_1 \varepsilon_1 \rho_1 A(1-\phi)zr_1 - 3\eta_2 \varepsilon_2 \rho_2 A(1-\phi)zr_2 \tag{11}$$

$$\frac{dF_{C_6H_6}}{dZ} = -\eta_2 \varepsilon_2 \rho_2 A(1-\phi)zr_2 \tag{12}$$

$$\frac{dF_{C_6H_{12}}}{dZ} = \eta_2 \varepsilon_2 \rho_2 A(1-\phi)zr_2 \tag{13}$$

The Ergun momentum balance equation is used to give the pressure drop along the reactor:

$$\frac{dP}{dZ} = -10^{-5} \frac{(1-\phi)G^o z}{d_P \varepsilon^3 \rho_G g_c} \left[\frac{150\mu_G(1-\phi)}{d_P} + 1.75G^o\right] \tag{14}$$

where ε_k is the volume fraction of catalyst k and is given by:

$$\varepsilon_k = \frac{\text{volume of catalyst } k \text{ in a well mixed catalyst bed}}{\text{volume of a well mixed catalyst bed}},$$
$$k = 1, 2 \tag{15}$$

Exit gas

Feed gas

Figure 1 Schematic representation of the fixed bed reactor with a well-mixed catalyst pattern.

The fractional conversions of C_8H_{10} and C_6H_6 are given by:

$$X_{C_8H_{10}} = \frac{F^o_{C_8H_{10}} - F_{C_8H_{10}}}{F^o_{C_8H_{10}}} \tag{16}$$

$$X_{C_6H_6} = \frac{F^o_{C_6H_6} - F_{C_6H_6}}{F^o_{C_6H_6}} \tag{17}$$

3.2. The dusty gas model for the catalyst pellet

The catalyst pellet governing equations are developed based on the dusty gas model using the following assumptions:

1. The catalyst pellet is assumed to be at isothermal steady state conditions.
2. The external mass and heat transfer resistances are assumed to be negligible.
3. The concentration profiles are symmetrical about the center of the pellet.
4. The ideal gas behavior is assumed.

The intraparticle molar balance differential equations are expressed as follows:

For catalyst 1:

$$\frac{dN^1_{C_8H_{10}}}{dl} = -\rho_1 r_1 \tag{18}$$

$$\frac{dN^1_{C_8H_8}}{dl} = \rho_1 r_1 \tag{19}$$

$$\frac{dN^1_{H_2}}{dl} = \rho_1 r_1 \tag{20}$$

$$N^1_{C_6H_6} = N^S_{C_6H_6} \tag{21}$$

$$N^1_{C_6H_{12}} = N^S_{C_6H_{12}} \tag{22}$$

For catalyst 2:

$$\frac{dN_{C_6H_6}^2}{dl} = -\rho_2 r_2 \qquad (23)$$

$$\frac{dN_{H_2}^2}{dl} = -3\rho_2 r_2 \qquad (24)$$

$$\frac{dN_{C_6H_{12}}^2}{dl} = \rho_2 r_2 \qquad (25)$$

$$N_{C_8H_{10}}^2 = N_{C_8H_{10}}^S \qquad (26)$$

$$N_{C_8H_8}^2 = N_{C_8H_8}^S \qquad (27)$$

By using the rigorous dusty gas model, the total diffusive flux can be written as (Mason and Malinauskas, 1983; Abashar, 1990):

$$-grad\, C_i = \frac{N_i}{D_{K_i}^e} + \sum_{\substack{j=1 \\ i \neq j}}^{n=5} \frac{y_j N_i - y_i N_j}{D_{ij}^e}, \quad i = 1\text{--}5 \qquad (28)$$

with the following boundary conditions:

$$\begin{aligned} l &= 0, \quad N_i = 0 \\ l &= L_c, \quad C_i = C_i^s, \quad i = 1\text{--}5 \end{aligned} \qquad (29)$$

The components are denoted by: 1 for C_8H_{10}, 2 for C_8H_8, 3 for H_2, 4 for C_6H_6, and 5 for C_6H_{12}. The characteristic length L_c is given by (Aris, 1957):

$$L_c = \frac{V_P}{S_P} \qquad (30)$$

where V_P and S_P are the volume and external surface area of the catalyst pellet.

The effective diffusivity of any component (D_i^e) can be obtained from Eq. (28) by dividing its flux by the negative of its concentration gradient

$$\frac{-grad\, C_i}{N_i} = \frac{1}{D_i^e} = \frac{1}{D_{K_i}^e} + \sum_{\substack{j=1 \\ i \neq j}}^{n=5} \frac{y_j - y_i(N_j/N_i)}{D_{ij}^e}, \quad i = 1\text{--}5 \qquad (31)$$

from Eq. (31):

$$N_i = D_i^e(-grad\, C_i), \quad i = 1\text{--}5 \qquad (32)$$

The effectiveness for reaction j is given by:

$$\eta_j = \frac{\int_0^{L_c} r_j\, dL}{L_c r_j^s}, \quad j = 1, 2 \qquad (33)$$

3.3. Numerical solution

The ordinary differential equations of the bulk gas phase are integrated by an IMSL subroutine (DGEAR) based on a Runge–Kutta–Verner fifth and sixth-order method with automatic step size and double precision to ensure accuracy. The catalyst pellet equations resulting from using the dusty gas model are forming a two-point boundary value problem and solved by the global orthogonal collocation technique (Villadsen and Michelsen, 1978). Details of the efficient computation algorithm developed for the dusty gas model is given elsewhere (Abashar, 1990).

4. Results and discussion

The fixed bed catalytic reactor with well-mixed catalysts pattern configuration is loaded with two distinct discrete types of pellets that are physical well mixed as shown in Fig. 1. The data used for this simulation study is shown in Table 1.

In order to distinguish between the catalysts employed in this investigation, the catalyst used for dehydrogenation of ethylbenzene (the primary reaction) is considered to be catalyst 1 and that used for the hydrogenation of benzene (the auxiliary reaction) is catalyst 2.

Fig. 2 shows the performance of the fixed bed reactor with auxiliary reaction (FBRAR) that contains well mixed catalysts compared to the conversion of ethylbenzene obtained along the length of the fixed bed reactor (FBR). For the FBRAR the composition of the reactor bed is ($\varepsilon_1 = 0.85$, $\varepsilon_2 = 0.15$). As it can be seen the FBR reaches the equilibrium conversion of 37.29% at the beginning of the reactor at a dimensionless reactor length of 0.102, i.e., 10.2% from the total length of the reactor. The reaction is severely limited by thermodynamic equilibrium and only small part of the reactor is utilized. It is clear that the auxiliary reaction has significant effect on the displacement of the thermodynamic equilibrium and the substantial improvement of the performance of the FBRAR is obvious by the 100% conversion of ethylbenzene achieved. This significant displacement of the thermodynamic equilibrium is achieved due to the influence of hydrogen removal from the reaction medium by the auxiliary reaction (reaction
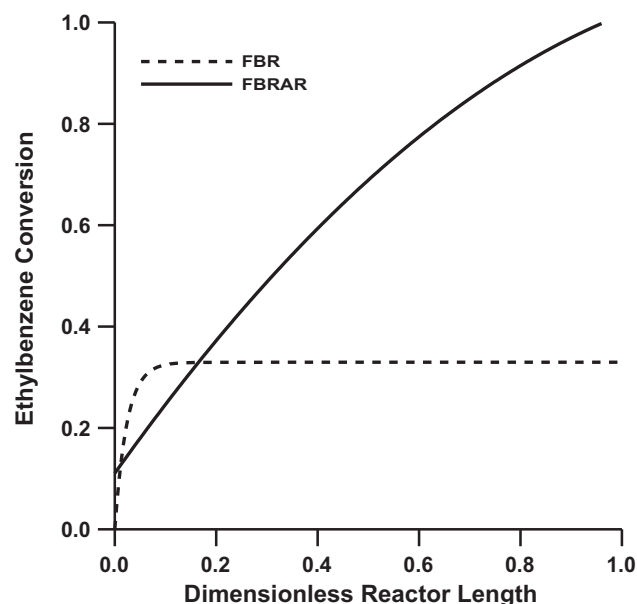
Figure 2 Ethylbenzene conversion profiles in the FBR and FBRAR.

Table 1	Data for the simulation.
Reactor length	1.0 m
Reactor diameter	2.5×10^{-2} m
Catalyst pellet diameter	4.0×10^{-3} m
Porosity of catalyst bed	0.5
Catalyst 1 bulk density	1400 kg/m^3
Catalyst 2 bulk density	1200 kg/m^3

(2)), i.e., reaction (1) is thermodynamically favored by the removal of hydrogen product in the forward direction according to Le Chatelier's principle. From the kinetic point of view the reduction of partial pressure of hydrogen due to the removal of hydrogen from the reaction medium increases the rate of consumption of ethylbenzene as shown by Eq. (2). Fig. 3 shows that, also 100% conversion of benzene is attained by the FBRAR.

Fig. 4 shows the ethylbenzene conversion profiles along the FBRAR for low concentrations of catalyst 2 ($\varepsilon_2 = 0.00, 0.04$ and 0.06). As it can be seen that, the addition of small amount of catalyst 2 to the bed has significant impact on improving the ethylbenzene conversion. Fig. 5 shows the ethylbenzene conversion profiles along the FBRAR for high concentrations of catalyst 2 ($\varepsilon_2 = 0.4, 0.7$ and 0.9). It is clearly shown that the increase of catalyst 2 in the bed to high concentration causes
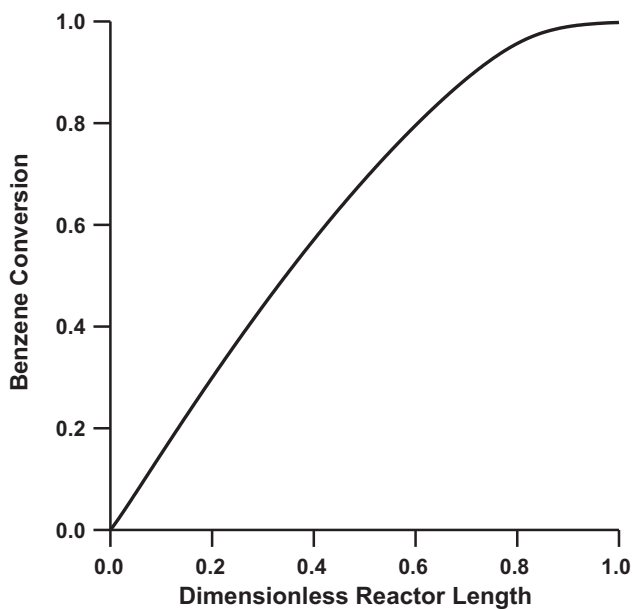
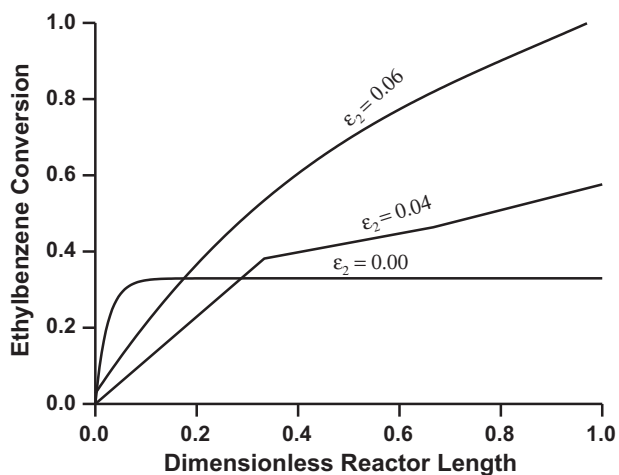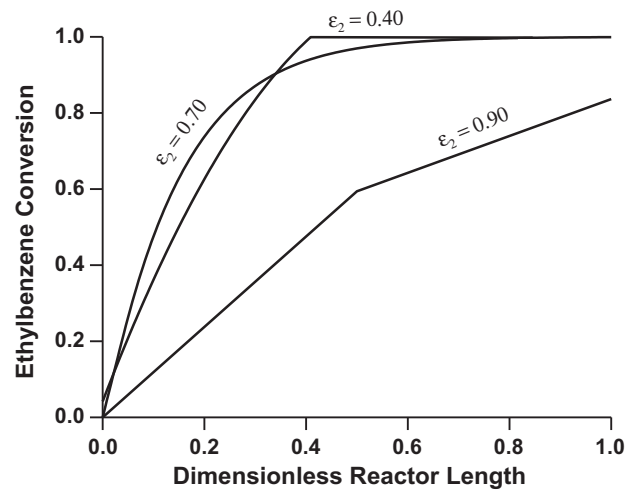**Figure 5** Ethylbenzene conversion profiles along the FBRAR for high concentration of catalyst 2.

significant drop in the exit ethylbenzene conversion. This drop due to the fact that the increase of catalyst 2 in the bed at the expense of catalyst 1 in the bed. This important result implies that the composition of the bed should be optimized.

Fig. 6 shows the exit ethylbenzene conversion varies as a function of the bed composition for several different feed pressures at relatively low temperature of 700.0 K. All profiles show optimum values as the concentration of catalyst 2 increases. The optimum ethylbenzene conversion increases from 42.32% to 57.69% as the feed pressure increases from 70 to 512.0 kPa, respectively.

Fig. 7 shows the exit ethylbenzene conversion varies as a function of the bed composition for several different feed pressures at a relatively high temperature of 900.0 K. In this case the profiles form plateaus of 100% conversion of ethylbenzene.
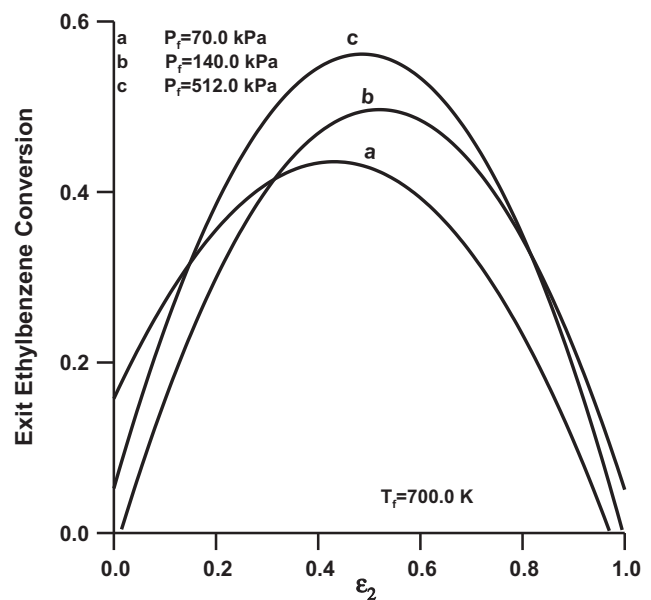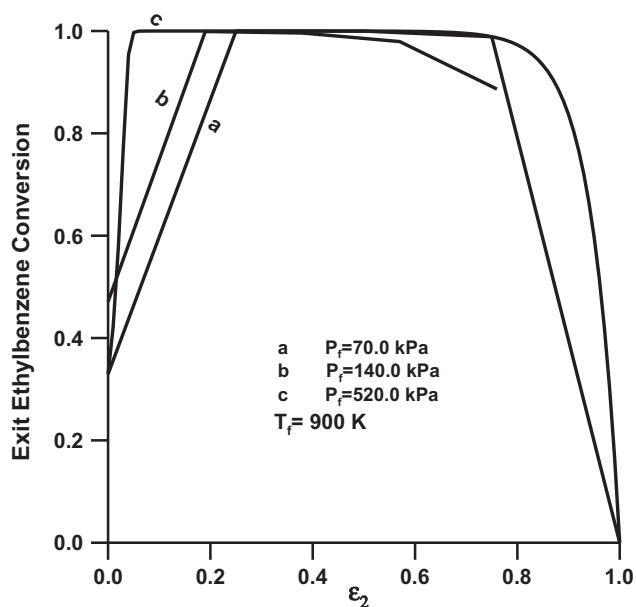
Figure 3 Benzene conversion profile along the FBRAR.

Figure 4 Ethylbenzene conversion profiles along the FBRAR for low concentration of catalyst 2.

Figure 6 Exit ethylbenzene conversion vs. catalyst 2 concentration for several feed pressures at 700 K.
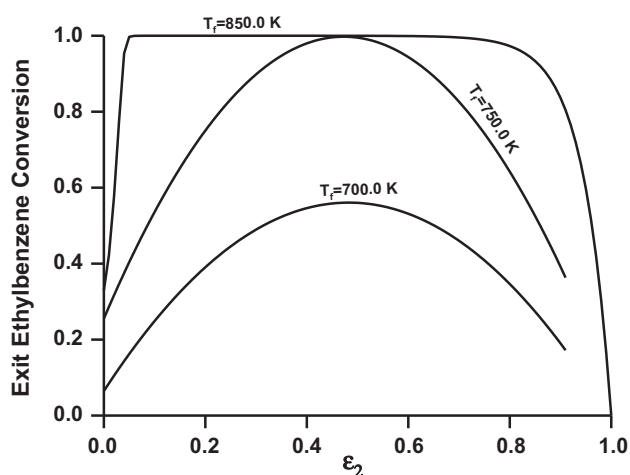
Figure 7 Exit ethylbenzene conversion vs. catalyst 2 concentration for several feed pressures at 900 K.

It is clear from Figs. 6 and 7 that the feed pressure has a pronounced effect on the exit ethylbenzene conversion.
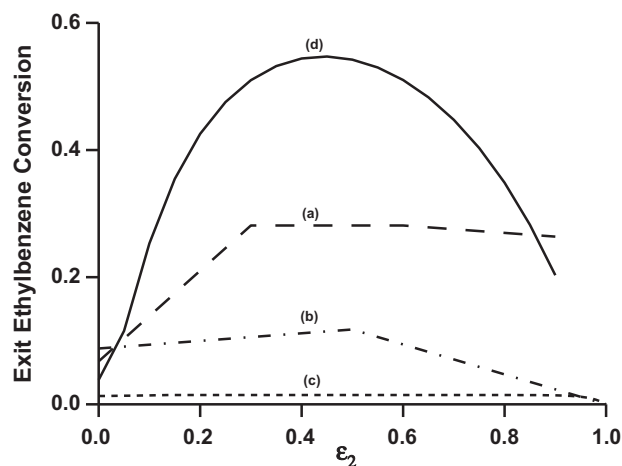
The exit ethylbenzene conversion varies as a function of the bed composition for several different feed temperatures (700, 750 and 850 K) is shown in Fig. 8. It is clearly shown that 100% conversion of ethylbenzene is achieved at temperatures of 750 and 850 K. At 700 and 750 K (relatively low temperatures) the exit conversion forms an optimum value. The results presented in this figure indicate the strong effect of feed temperature on the exit ethylbenzene conversion.

The effect of feed composition and catalyst 2 concentrations on the exit ethylbenzene conversion at 700 K and 140 kPa is shown in Fig. 9. Four feed compositions ((a)–(d)) are tested. The feed compositions are presented in Table 2.

The first feed composition (a) is rich in ethylbenzene and lean in benzene and hydrogen. The second feed composition
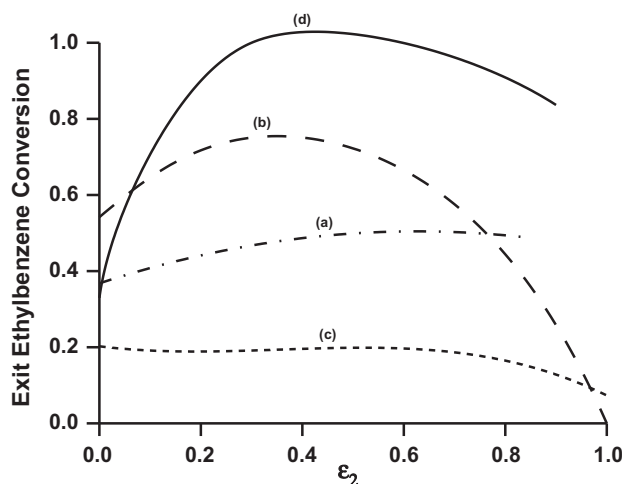

Figure 9 Effect of feed composition and catalyst 2 concentration on the exit ethylbenzene conversion at 700 K and 140 kPa.

(b) is rich in benzene and lean in ethylbenzene and hydrogen. The third feed composition (c) is rich in hydrogen and lean in ethylbenzene and benzene. For the fourth composition (case (d)), the molar feed composition is 34 mol% ethylbenzene, 33 mol% benzene and 33 mol% hydrogen, respectively. These components are reactants for reactions (1) and (2), and their selected composition of relatively equal amounts gives them fair contribution in participating in their corresponding reactions. As it can be seen the composition (d) gives the best per-

Table 2 Various feed compositions.

Component	Feed composition (mol%)			
	(a)	(b)	(c)	(d)
Ethylbenzene	70	15	15	34
Benzene	15	70	15	33
Hydrogen	15	15	70	33

Figure 8 Exit ethylbenzene conversion vs. catalyst 2 concentration for several feed temperatures at 250.0 kPa.

Figure 10 Effect of catalyst 2 concentration and feed composition on exit ethylbenzene conversion at 900 K and 140 kPa.

formance among the four feed compositions and also shows an optimum value at $\varepsilon_2 = 0.431$.

Fig. 10 shows the effect of feed composition and catalyst 2 concentration on the exit ethylbenzene conversion at 900 K and 140 kPa. It is clearly shown that the increase of the feed temperature favors the performance of the four feed compositions and the feed composition (d) achieves 100% exit ethylbenzene conversion. Also the temperature has strong influence on the feed composition (b).

As it has been shown in Figs. 5, 7, 8 and 10, there is a wide range of bed composition, which gives 100% conversion of ethylbenzene at different operating conditions and reactor lengths and in some cases far from the reactor exit, i.e., at shorter reactor lengths. Therefore, in order to investigate the reactor performance in a unified way, we defined a dimensionless effective reactor length (L_{eff}) as the length of the reactor that gives 99.9% conversion of ethylbenzene. Fig. 11 shows the effective reactor length versus bed composition at 900.0 K. It is shown that the effective length passes through a minimum with increasing the concentration of catalyst 2 in the bed. The occurrence of the minimum could be due to the interaction of many factors such as the concentration of the catalysts in the bed, temperature, pressure and the thermodynamic equilibrium. This result indicates that the composition of the catalyst bed should be controlled carefully.

Sensitivity analysis for the effect of feed pressure and catalyst 2 concentration on the dimensionless effective reactor length at low temperature of 700 K is shown in Fig. 12. It is clear that the pressure has significant effect on the dimensionless effective reactor length.

Fig. 13 shows sensitivity analysis for the effect of feed pressure and catalyst 2 concentration on the dimensionless effective reactor length at a temperature of 900 K. It is clear shown that the increase of the temperature from 700 to 900 K affects the position of the minima.

Sensitivity analysis for the effect of the feed temperature on the effective reactor length as a function of bed composition at
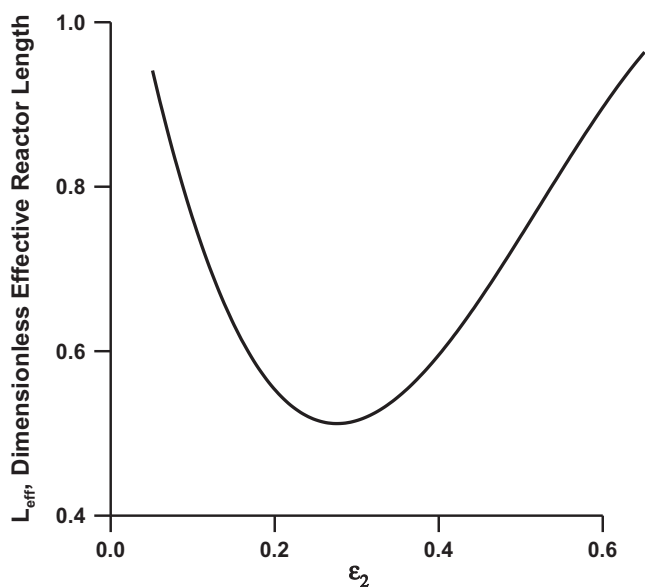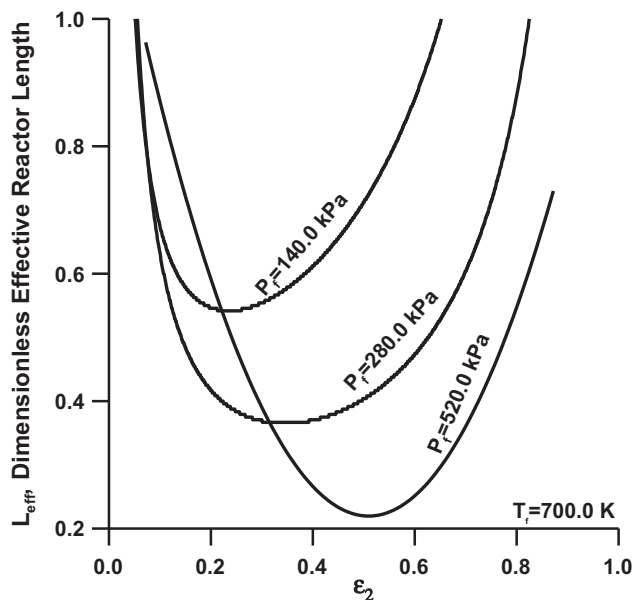

Figure 12 Effect of feed pressure and catalyst 2 concentration on the dimensionless effective reactor length at low temperature of 700 K.

$P_f = 280$ and 520 kPa are shown in Figs. 14 and 15, respectively. As it can be seen that for each temperature there is a range of bed composition in which the effective length is satisfied. Within the start and the end of each range there is an optimum effective length. Increasing the temperature causes a significant decrease in the optimum effective length. It is interesting that at the operating pressure of 280 kPa the increase in temperature seems to shift the optimum value of the dimensionless effective length to the left, i.e., towards low concentration of catalyst 2 as shown in Fig. 14, while at the operating pressure of 520 kPa the increase in temperature has an oppo-
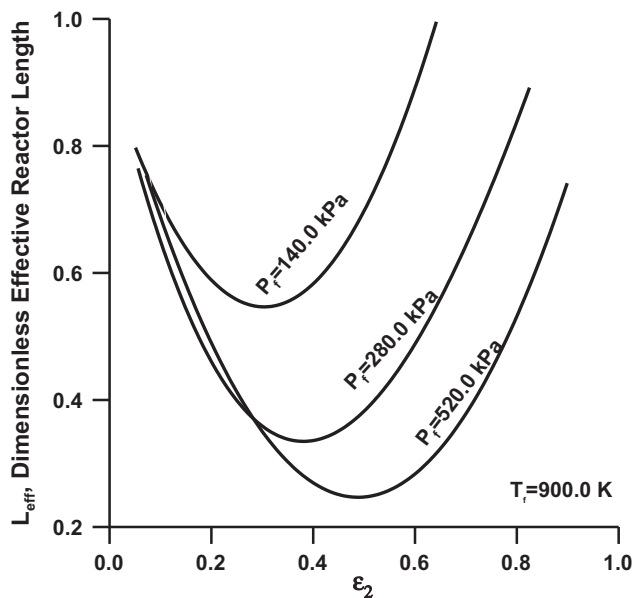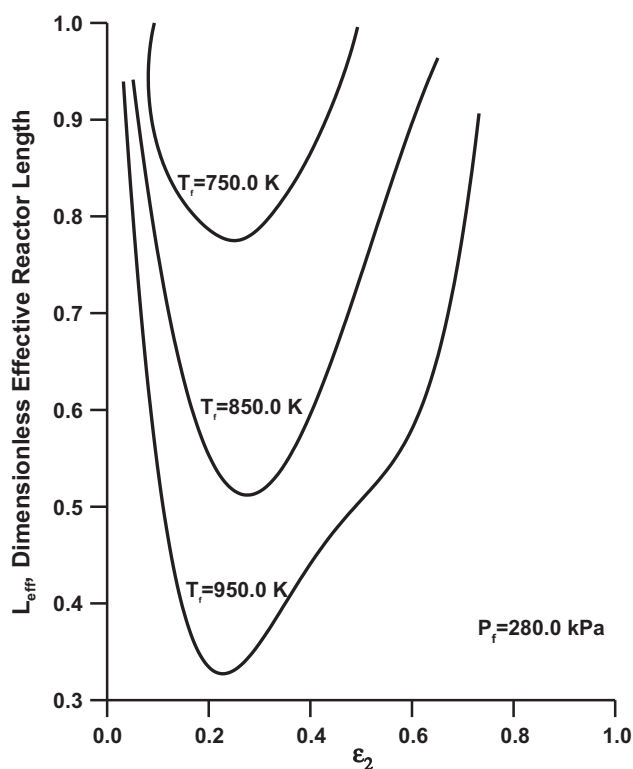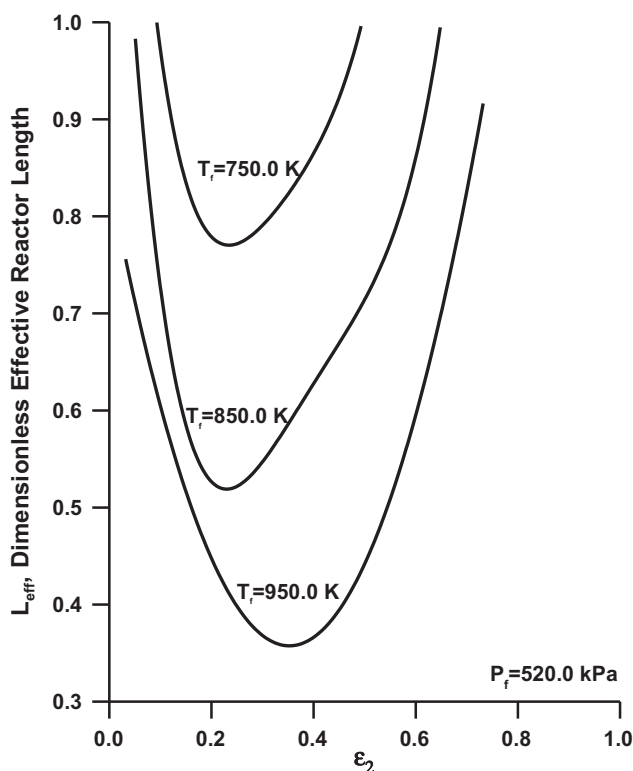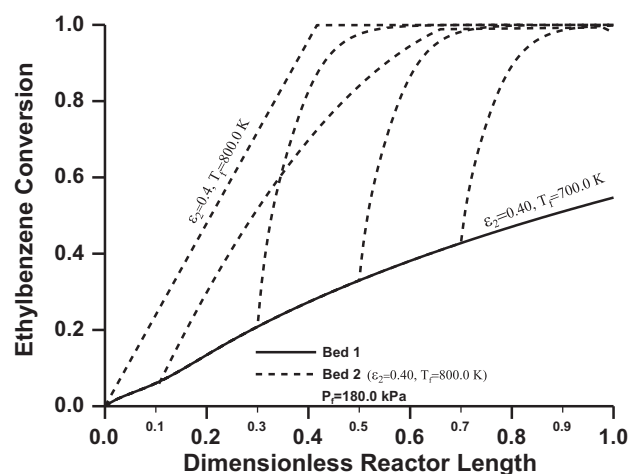

Figure 11 Dimensionless effective reactor length as a function of catalyst 2 concentration.

Figure 13 Effect of feed pressure and catalyst 2 concentration on the dimensionless effective reactor length at low temperature of 900 K.

Figure 14 Effect of feed temperature and catalyst 2 concentration on the dimensionless effective reactor length at $P_f = 280$ kPa.


Figure 15 Effect of feed temperature and catalyst 2 concentration on the dimensionless effective reactor length at $P_f = 520$ kPa.

Figure 16 Two beds at 700.0 and 800.0 K.

site effect of shifting the optimum value of the dimensionless effective reactor length to the right, i.e., towards high concentration of catalyst 2 as shown in Fig. 15.

In order to investigate the effect of switching between low and high temperature beds, the reactor is divided into two beds. The first bed is kept at 700.0 K and the second bed at 800.0 K. Four volume configurations having volume fractions of 0.1, 0.3, 0.5 and 0.7 for bed 1 are considered. It is clearly shown in Fig. 16, that for all configurations the switching policy achieves almost 100% conversion of ethylbenzene. The volume fraction configuration of 0.7 shows the best configuration with respect to thermal characteristics since it is possible to achieve high conversion of ethylbenzene by switching from a long bed at low temperature to a short bed at high temperature. This is very interesting results, since it is known that excessive temperatures have destructive effects on the catalysts and the mechanical stability of the reactors. Moreover, the energy operating cost is high at elevated temperatures. On the other hand the other three volume fraction configurations (0.1, 0.3 and 0.5) achieve high conversion of ethylbenzene at shorter total reactor length which may decrease the fixed cost. The volume fraction configuration of 0.3 gives better perfor-
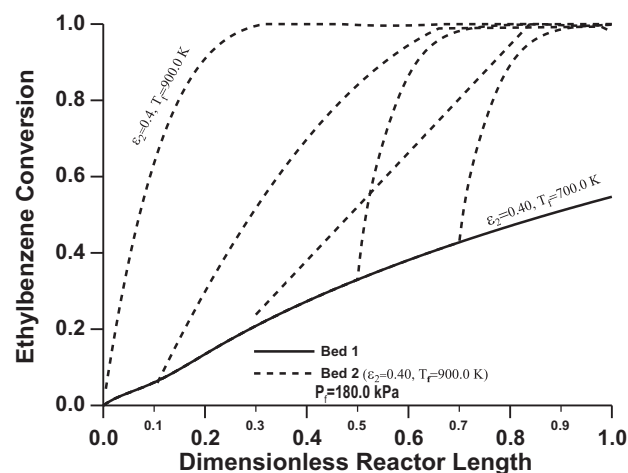
Figure 17 Two beds at 700.0 and 900.0 K.

mance than the configuration of 0.1 volume fraction with respect to the total reactor length. The temperature of the second bed is further increased to 900 K and the results are presented in Fig. 17. In this case the volume fraction configuration of 0.1 gives better performance than the rest volume fraction configurations with respect to the total reactor length. Also in this case, the volume fraction configuration of 0.7 gives the best configuration with respect to thermal characteristics since shift from low temperature to high temperature can be achieved through a longer first bed and a shorter second bed.

5. Conclusions

A rigorous steady state mathematical model based on the dusty gas model is implemented to investigate the performance of a novel reactor for efficient simultaneous production of styrene and cyclohexane by reaction coupling of ethylbenzene dehydrogenation with benzene hydrogenation. In the range of the parameters investigated, the simulation results reveal that the introduction of the concept of dual-functionality of the well-mixed catalyst bed has substantial increases in the conversion of ethylbenzene and benzene (almost 100%) via thermodynamic equilibrium displacement. It is found that substantial decrease in the reactor length is achievable by employing a reactor catalyst bed with different bed composition. Effective operating regions with optimal conditions are observed. An effective reactor length criterion is used to evaluate the performance of the reactor under these optimal conditions. The effective reactor length is found to be sensitive and favored by high feed temperature and pressure. It was also found that the increase of feed pressure affects the position of the minima of the dimensionless effective reactor length at different feed temperatures. This shift of the minima could be due to the complex interaction of the feed pressure with many factors such as the concentration of the catalysts in the bed, the thermodynamic equilibrium and the kinetics. The results also suggest that 100% conversion of ethylbenzene and benzene at low temperature and shorter reactor length can be achieved by maintaining the reactor beds at different temperatures. This is very interesting results, since it is known that excessive temperatures have destructive effects on the catalysts, the mechanical stability of the reactors and the energy operating cost is high at elevated temperatures. Moreover, these results also imply that appreciable energy saving can be realized by this reactor bed switching configurations. The mathematical model results presented in this paper can be validated by an experimental investigation that can be carried out in a bench scale fixed bed reactor of 1 m in length and 2.5 cm in diameter. Two well-mixed catalysts should be loaded into the reactor. Iron-promoted catalyst for the dehydrogenation of ethylbenzene to styrene (reaction (1)) and nickel catalyst for hydrogenation of benzene (reaction (2)). This well-mixed catalyst pattern can be made of composite pellets, i.e., the two catalysts are co-extruded into composite pellets or two discrete types of pellets that are physically well-mixed. This type of experimental setup is suitable to test the range of key parameters of feed temperature, pressure, and the bed composition presented in this paper. Future research should focus on different catalyst layer configurations and rigorous optimization studies.

References

Abashar, M.E.E., 1990. Modeling and Simulation of Industrial Natural Gas Steam Reformers and Methanators Using the Dusty Gas Model. M.Sc. Thesis, University of Salford, UK.

Abashar, M.E.E., 2002a. Integrated membrane reactors with oxygen input for dehydrogenation of ethylbenzene to styrene. In: Proceedings of the Regional Symposium on Chemical Engineering (RSCE) and 16th Symposium of Malaysian Chemical Engineers (SOM-ChE), Malaysia, p. 1231.

Abashar, M.E.E., 2002b. Integrated catalytic membrane reactors for decomposition of ammonia. Chem. Eng. Proc. 41, 403–412.

Abashar, M.E.E., Al-Sughair, Y.S., Al-Mutaz, I.S., 2002. Investigation of low temperature decomposition of ammonia using spatially patterned catalytic membrane reactors. Appl. Catal. A: Gen. 236, 35–53.

Abdalla, B.K., Elnashaie, S.S.E.H., 1993. A membrane reactor for the production of styrene from ethylbenzene. J. Membr. Sci. 85, 229.

Aris, R., 1957. On shape factors for irregular particles. I. The steady state problem, diffusion and reaction. Chem. Eng. Sci. 6, 262–265.

Becker, Y.L., Dixon, A.G., Moser, W.R., Ma, Y.H., 1993. Modeling of ethylbenzene dehydrogenation in a catalytic membrane reactor. J. Membr. Sci. 77, 233–244.

Cote, A.S., Deglass, W.N., Ramkrishna, D., 1999. Investigation of spatially patterned catalytic reactors. Chem. Eng. Sci. 54, 2627–2635.

Dittmeyer, R., Höllein, V., Quicker, P., Emig, G., Hausinger, G., Schmidt, F., 1999. Factors controlling the performance of catalytic dehydrogenation of ethylbenzene in palladium composite membrane reactors. Chem. Eng. Sci. 54, 1431–1439.

Elnashaie, S.S.E.H., Abdallah, B.K., Elshishini, S.S., Alkhowaiter, S., Noureldeen, M.B., Alsoudani, T., 2001. On the link between intrinsic catalytic reactions kinetics and the development of catalytic processes. Catalytic dehydrogenation of ethylbenzene to styrene. Catal. Today 64, 151–162.

Gobina, E., Hou, K., Hughes, R., 1995. Mathematical analysis of ethylbenzene dehydrogenation: comparison of microporous and dense membrane systems. J. Membr. Sci. 105, 163–176.

Marangozis, J.K., Mantzouranis, B.G., Sophos, A.N., 1979. Intrinsic kinetics of hydrogenation of benzene on nickel catalyst supported on kieselguhr. Ind. Eng. Chem. Prod. Res. Dev. 18, 61–73.

Mason, E.A., Malinauskas, A.P., 1983. Gas Transport in Porous Media: The Dusty Gas Model. Elsevier, Amsterdam.

Moustafa, T.M., Elnashaie, S.S.E.H., 2000. Simultaneous production of styrene and cyclohexane in an integrated membrane reactor. J. Membr. Sci. 178, 171–184.

Sheel, C.G.P., Crowe, C.M., 1969. Simulation and optimization of an existing ethylbenzene dehydrogenation reactor. Can. J. Chem. Eng. 47, 183–192.

Villadsen, J., Michelsen, M.L., 1978. Solution of Differential Equation Models by Polynomial Approximation. Prentice-Hall Inc., New Jersey.